euspen's 22nd International Conference & Exhibition, Geneva, CH, May/June 2022
www.euspen.eu

Frequency scanning interferometry for accurate robot position measurement

Mohammed A. Isa[1], Mojtaba A. Khanesar[1], Richard Leach[1, 2], David Branson[1], and Samanta Piano[1]

[1]*Manufacturing Metrology Team, Faculty of Engineering, University of Nottingham, Nottingham, UK*
[2]*Taraz Metrology, Nottingham, UK*

mohammed.isa@nottingham.ac.uk

Abstract
This paper presents a frequency scanning interferometry (FSI) shortwave infrared (IR) setup developed for position and orientation measurement of industrial robots. Within contemporary and future industrial frameworks, robots—in particular collaborative robots (cobots)—will play an important role in ensuring safe and coherent automation of manufacturing processes. Robots are generally regarded as a means to improve performance and reduce production costs through improved production efficiency, versatility and adaptability. However, due to high flexibility and compliance imposed for safety reasons, exact coordinate positions of robots during operation can vary significantly from desired positions. Systematic positioning errors are further exacerbated by backlash from wear and tear in motors and motion joints. Accurate measurement feedback is therefore required to satisfy performance requirements in high-accuracy applications. Common state-of-the-art solutions for high-accuracy applications involve the use of either costly laser tracking systems or less accurate photogrammetric systems. FSI can provide an alternative metrological solution for the measurement of position feedback for robots. Unlike conventional interferometry that measures relative displacements, FSI can be used for absolute distance measurement eliminating the need for continuous displacement of targets from reference positions during measurements. An optical fibre FSI setup has been developed to address requirements needed for measurement of robotic end-effector position and orientation. Some of the requirements considered include pose measurements, wide measurement field of view, sensitivity to moving targets and identification of multiple targets when displaced. Absolute distances of reflective targets mounted on the end-effector of a UR5 robot can be measured using frequency analysis of the interference intensity resulting from the interaction of frequency tuned IR light and the reflections of the light from the targets. Reflected light from each target interferes with a beat frequency that corresponds to the target distance. After target distances are determined from the beat frequencies, methods of determining robotic coordinate positions are investigated. Preliminary results indicate that real-time calibration of swept frequency using gas cell and frequency analysis of interference data are promising for robotic FSI position measurement. Future work will integrate the suitable elements of the FSI measurement systems for robotic tracking and comparative uncertainty analysis.

Keywords: Frequency scanning interferometry, position measurement, uncertainty

1. Frequency scanning interferometers

In classical displacement interferometers, interference is induced by the optical path difference of the reference and measurement beams. For a displacement interferometer, a measurement mirror is usually moved from a reference point to a target position without interruption of propagated beam. In several applications where multi-dimensional and absolute distance measurements are required, the use of a displacement interferometer is not feasible because of the requirement for continuous mirror displacement. Frequency scanning interferometry (FSI) presents an alternative strategy for inducing interference by variation of the frequency of the propagated beam. The variable frequency in FSI modulates absolute distance, making it possible to measure distance, rather than displacement, from the observed interference intensity of targets. Distances in FSI can be measured through phase-measurement or frequency spectrum analysis of interference signal [1]. Frequency-based FSI can measure multiple targets and when light intensity is relatively low [2].

Due to simplicity, most FSI systems use collimated beams with target mirrors constrained to one-directional movement. To measure robotic end-effector position and orientation, multi-dimensional distances to multiple retroreflective targets are required. Beams commonly collimated from fibre guides have narrow cross sections that cannot provide the coverage required for multi-target FSI. As a result, divergent multi-target FSI has been suggested using either a fibre ferrule tip [2] or a measurement head with a divergent lens [3]. In this paper, FSI configurations, requirements and position measurement options are studied for a robotic metrology application.

Section 2 summaries the principle of multi-target FSI, accurate frequency calibration and the FSI setup. Section 3 discusses how FSI distances can be used to measure robotic position and orientation. Finally, section 4 gives preliminary results and discusses future work.

2. Multi-target FSI methodology

Consider a frequency tuned laser light at time t, with initial frequency ν_0 (at time $t = 0$), that mixes with reflected light returning from m retroreflective targets, after the light travel times $\tau_i|_{i=1,2\ldots m}$. The observed intensity of interference if the light is linearly swept to a new frequency $\nu(t) = \nu_0 + \alpha t$, at time t, is given by

$$I(t) = \sum_{i=1}^{m} A_i cos[2\pi(\alpha\tau_i t + \nu_0\,\tau_i)], \qquad (1)$$

where A_i is the signal magnitude caused by each target. The frequency scan rate α in equation (1) can be set from the tuneable laser and is assumed to be constant. When working in the wavelength domain, the wavelength scan rate can be

determined from the frequency scan rate: $\alpha_\lambda = \frac{\partial\lambda}{\partial x} = -\frac{\lambda}{\nu}\alpha$. Tuneable laser sources have limitations that result in scan rates varying slightly during each sweep [4]. To make accurate measurements, the accurate value of the instantaneous scan frequency (or wavelength) needs to be measured.

Frequency-based FSI is suitable for multi-target measurements because each target will have a corresponding peak beat frequency f_i when the fast Fourier transform (FFT) of the observed intensity is evaluated. Distances to measured retroreflectors $d_i|_{i=1,2\ldots m}$ can be determined from

$$d_i = \frac{cf_i}{2n\alpha}, \qquad (2)$$

where n is the refractive index of the medium. The reference interferometer distance is also related by the same relationship given in equation (2). Since the reference distance is commonly more stable than the measurement distances, fluctuations in the reference beat frequency can be used to mitigate the effects of non-linearity of frequency sweep.

2.1. Frequency calibration and data processing

The frequency (or wavelength) of tuned laser light is calibrated using a NIST hydrogen cyanide calibration standard SRM 2519a. The calibration standard is based on the fundamental molecular absorption lines that are shown in Figure 1. Accurate wavelengths (with combined uncertainties of less than 0.2 pm using a coverage factor $k = 2$) at 54 absorption lines are given in the calibration certificate [5]. When the measured photodetector signal of the frequency calibration channel in Figure 2 is observed, the signal should have a similar set of absorption lines as the certificate. By comparing the line spacings of the signal with the standard, the linearity of the laser sweep can be determined.

Real-time signal data then needs to be processed and synchronised with the laser source. The laser source used in this paper provides trigger signals at the start and stop time of sweeping cycles, helping to provide precise data windows to detect the gas absorption lines and perform distance measurements. Since the beat periods are typically less than the sweeping time for targets at close range, it is possible to measure multiple distances in a single sweep. However, the accuracy of the distance measurements will depend on how accurate the gas cell absorption lines are calibrated for a partial sweep. There are series of data manipulations, such as filtering and interpolations that can improve measurements [6]. Gas cell signals are filtered and interpolated to detect absorption peaks in this paper.

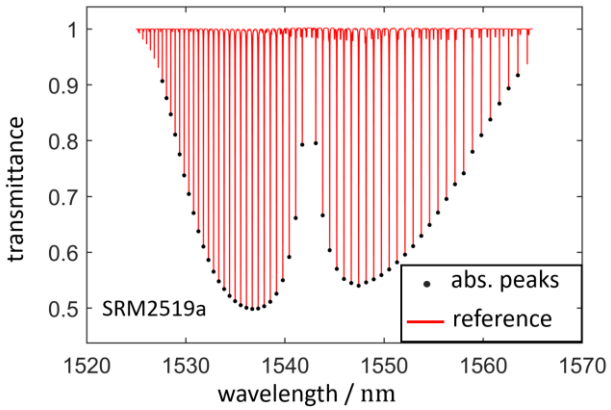

Figure 1. Hydrogen cyanide reference transmittance spectrum showing absorption lines and detected absorption peaks.

2.2. Multi-target FSI setup

A 1 mW tuneable laser is used to sweep light from 1525 nm to 1565 nm at a rate of up to 2000 nm/s. The fibre-coupled light is distributed to a reference interferometer, a gas cell and several measurement interferometers in parallel. Photodetectors are used for real-time measurement of both the intensities of the interferometric channels and the transmission intensity of the gas cell. Interference is established by mixing the emitted light with the reflected light from retroreflective targets. The light going to the measurement channels is amplified by an erbium-doped fibre amplifier (EDFA) to provide sufficient intensity of received back-reflected light from the targets.

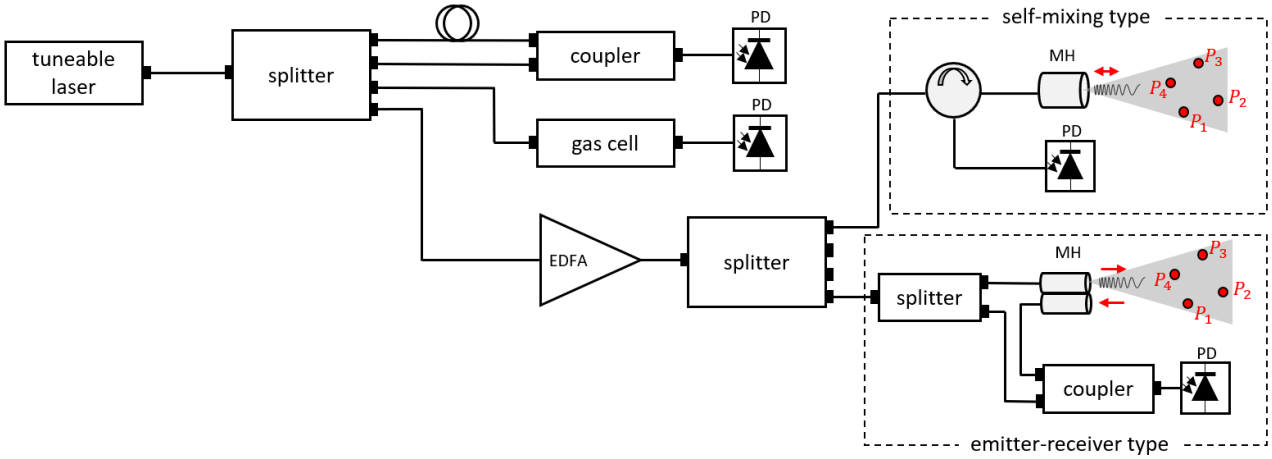

Figure 2. FSI system showing interferometer and frequency calibration (using gas cell) channels connected to a source tuneable laser with photodetector (PD) outputs. Additional measurement interferometers can be attached to the splitter. Self-mixing type and emitter-receiver type measurement heads (MHs) are used in the measurement interferometer channels.

Two types of light mixing methods for the measurement interferometer are shown in Figure 2: self-mixing and emitter-receiver type mixing. In the self-mixing interferometer, emitted light is split at the exit of the measurement head. The split beam bounces back and is interfered with the returning light from the retroreflectors. The flat surface of the ferrule tip of FC/PC type fibre connector end can be used as a cheap beam splitter and the numerical aperture (NA) of the optical fibre defines the beam divergence [2]. Alternatively, a fibre-coupled beam diverging lens could be attached to the fibre for better divergence. The critical limitation of divergent-beam FSI is the measurement limited range (around 0.3 m at a maximum eye-safe power [3]) of the measurement heads. At the cost of a more complex optical path length, an emitter-receiver type

interferometer can be used. The optics of the emitter and receiver can be designed separately to improve measurement range and transmission efficiency. As a practical solution for the limited range of FSI, robotic positions at longer ranges can be measured using photogrammetry [7]. Figure 3 shows FSI targets and photogrammetric artefacts attached to a robotic end-effector. The accurate positioning of robots is more critical towards the end of desired trajectory in many industrial applications [8]. At these near end positions, movement of the robot is expected to be slow and dynamic issues of FSI can be reduced and accuracy maintained. Therefore, less accurate measurements using photogrammetry can be applied before reaching close to the final positions of a desired trajectory. Research on implementation of photogrammetry for robotic tracking is ongoing, but intelligent integration of photogrammetry and FSI should improve robotic metrology.

3. Position measurement

Distances evaluated from FSI can be used to determine the three-dimensional (3D) positions of target reflectors through an analysis of the rigid body kinematics of the placed targets. Given a rigid target reflector network, methods for evaluating 3D positions using a system with two to four measurement heads are discussed.

3.1. Position using two measurement heads

Coordinate positions of the rigid points $\boldsymbol{P}_1(x_1, y_1, z_1)$, $\boldsymbol{P}_2(x_2, y_2, z_2)$, $\boldsymbol{P}_3(x_3, y_3, z_3)$ in Figure 3 can be determined from FSI distances computed from two measurement heads.

The origin of the coordinate frame is taken as the first measurement head position $\boldsymbol{A}$ and the direction of x-axis is along the second measurement head position $\boldsymbol{B}$(Figure 3). Finally, the z-axis is assigned such that the first point $\boldsymbol{P}_1$ lies on the xy plane (z_1 = 0). The 3D coordinate positions of the points can be evaluated given the rigid body spacings of the points ($d_{12} = \|\boldsymbol{P}_2 - \boldsymbol{P}_1\|$, $d_{13} = \|\boldsymbol{P}_3 - \boldsymbol{P}_1\|$, $d_{32} = \|\boldsymbol{P}_3 - \boldsymbol{P}_2\|$), the position of $\boldsymbol{B}(b, 0, 0)$ and the measured FSI distances from $\boldsymbol{A}$ and $\boldsymbol{B}$. If we assign the measured distances as $l_{A1} = \overline{\boldsymbol{AP}}_1$, $l_{A2} = \overline{\boldsymbol{AP}}_2$, $l_{A3} = \overline{\boldsymbol{AP}}_3$, $l_{B1} = \overline{\boldsymbol{BP}}_1$, $l_{B2} = \overline{\boldsymbol{BP}}_2$ and $l_{B3} = \overline{\boldsymbol{BP}}_3$, the coordinates can then be expressed as:

$$\left.\begin{aligned} z_1 &= 0 \\ x_1 &= \frac{1}{2}\left(\frac{l_{B1}^2 - l_{A1}^2}{s} - s\right); (s \neq 0) \\ x_2 &= \frac{1}{2}\left(\frac{l_{B2}^2 - l_{A2}^2}{s} - s\right); (s \neq 0) \\ x_3 &= \frac{1}{2}\left(\frac{l_{B3}^2 - l_{A3}^2}{s} - s\right); (s \neq 0) \\ y_1 &= \sqrt{l_{A1}^2 - x_1^2} \\ y_2 &= \frac{l_{A1}^2 + l_{A1}^2 - d_{12}^2 - 2x_1x_2}{2y_1}; (y_1 \neq 0) \\ z_2 &= \sqrt{l_{A2}^2 - x_2^2 - y_2^2} \\ y_3 &= \frac{(l_{A1}^2 + l_{A3}^2 - d_{13}^2 - 2x_1x_3)}{2y_1}; (y_1 \neq 0) \\ z_3 &= \frac{(l_{A2}^2 + l_{A3}^2 - d_{23}^2 - 2x_2x_3)}{2z_2} - \frac{y_2y_3}{z_2}; (z_2 \neq 0) \end{aligned}\right\}. \quad (2)$$

Equation (2) require a minimum of three matched target distances to be measured simultaneously. In addition, the coordinate positions are not defined at some target positions. Therefore, increasing the number of measurement heads can improve the likelihood of solving for the coordinate points as occlusions may also occur during operation.

3.2. Position measurement using trilateration

When a third measurement head is added at a position $\boldsymbol{C}$, the coordinate position of a target $\boldsymbol{P_i}(x_i, y_i, z_i)$ can be obtained from the distances $l_{Ai} = \overline{\boldsymbol{AP}}_i$, $l_{Bi} = \overline{\boldsymbol{BP}}_i$ and $l_{Bi} = \overline{\boldsymbol{BP}}_i$ measured from the measurement head positions $\boldsymbol{A}(x_A, y_A, z_A)$, $\boldsymbol{B}(x_B, y_B, z_B)$ and $\boldsymbol{C}(x_C, y_C, z_C)$ respectively. The coordinate position (x_i, y_i, z_i) can be evaluated by the equating to zero the following set of equations

$$\left.\begin{aligned} (x_i - x_A)^2 + (y_i - y_A)^2 + (z_i - z_A)^2 - l_{Ai}^2 &= 0 \\ (x_i - x_B)^2 + (y_i - y_B)^2 + (z_i - z_B)^2 - l_{Bi}^2 &= 0 \\ (x_i - x_C)^2 + (y_i - y_C)^2 + (z_i - z_C)^2 - l_{Ci}^2 &= 0 \end{aligned}\right\}. \quad (3)$$

The use of four measurement heads would further improve the accuracy of position measurements [9], by applying a multilateration method [10].

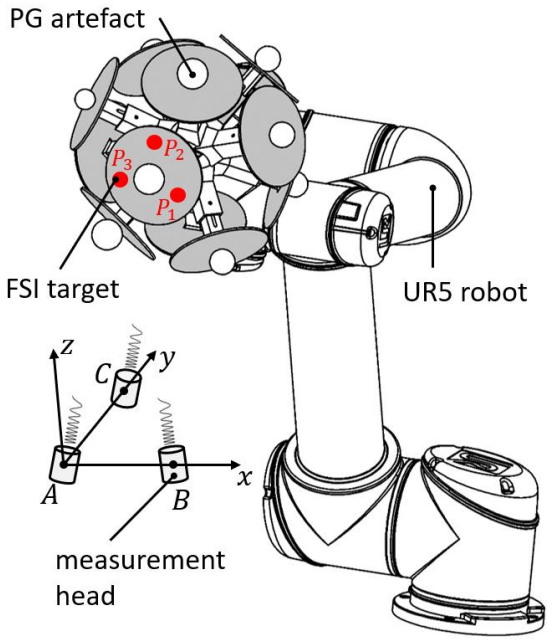

Figure 3. Robotic position measurement system showing rigid FSI retroreflective targets and photogrammetry (PG) artefacts.

4. Preliminary results

This section presents initial results of FSI signal processing and a simple multi-target FSI measurement result. Development of the robotic FSI system is on-going and the presented results are for investigation and validation of specific strategies to be implemented in the overall measurement system.

4.1. Frequency calibration and scan speed

Absorption lines are observed from the gas cell signal and the detected peaks are given in Figure 4. It was found that signal noise does not prevent detection of the absorption lines for wavelength calibration uncertainty of less than 30 pm [5]. Analogous peaks detected from the standard certificate data in Figure 1 are used to match the gas cell signal to the accurate time-dependent frequencies.

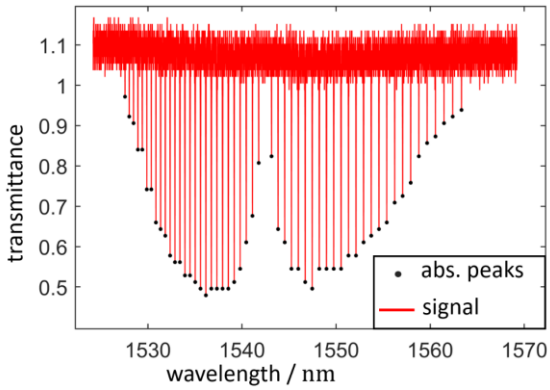

Figure 4. Gas cell absorption peaks detected from one sweep at wavelength scan rate of $1000\ \mathrm{nms}^{-1}$.

The calibrated wavelengths can be used to determine the actual scan speed of the laser. By using the spacing between the calibrated spectrum lines, the wavelength scan speed is evaluated and shown in Figure 5. It can be deduced that relying on the linearity of the laser scanning speed, without the calibration, can contribute significant error to measurements.

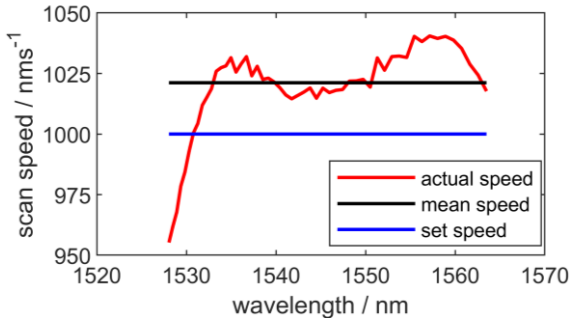

Figure 5. Comparison of tuneable laser wavelength scan rate for a setting of $1000\ \mathrm{nm\ s}^{-1}$.

4.2. Multi-target results

This section investigates the detectability of mixed beat intensity signals from the self-mixing interferometer presented in Section 2. As a result of safety requirements that are being put in place to run a class 3B EDFA amplifier, the robotic testing of the FSI interferometer could not be carried out. Therefore, unamplified 1 mW laser light is used to investigate interference signals in fibre patches connected by FC/PC type ferrule tips. The three ferrule targets T_1, T_2 and T_3 shown in Figure 6a) have reflectivities of about 4% that allow them to be used as splitters [2]. These reflected beams interfere with the beat frequencies given in Figure 6b). From this preliminary result, it is observed that beat frequencies are detectable even when the interfering light has power in the order of microwatts.

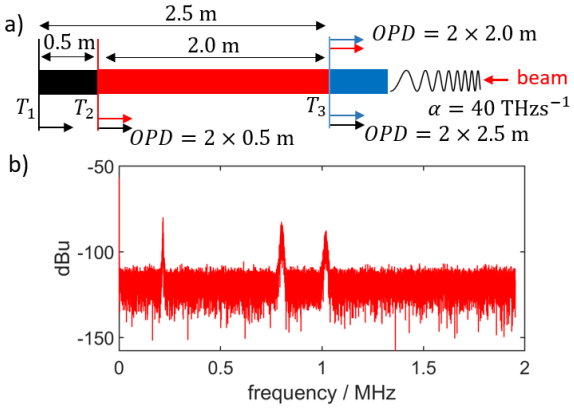

Figure 6. Multiple distance measurement and beat frequencies corresponding to each distance.

5. Conclusion and future work

With increasing autonomy and flexibility of robots, in-process and on-site applications of FSI should be investigated to extend robotic applications to accuracy-demanding industrial processes. FSI technology presents the opportunity to improve positional accuracy of robotic systems by providing interferometric measurement accuracy without relying on motion mechanisms that can contribute additional errors. The application of divergent beam for robotic FSI measurement is discussed, and preliminary results show that frequency analysis of the interference signals can detect distances at low light intensities. Future work will investigate FSI-based 3D coordinate measurement accuracy, integration with photogrammetry and tracking of robotic trajectories.

Acknowledgement: This work is funded by the Engineering and Physical Sciences Research Council (EPSRC) under grant number: EP/T023805/1 HARISOM. We further thank Mateusz Sosin (CERN) for his help.

References

[1] Warden M S 2014 Precision of frequency scanning interferometry distance measurements in the presence of noise *Appl. Opt.* **53** 5800–6

[2] Sosin M, Mainaud-Durand H, Rude V and Rutkowski J 2019 Frequency sweeping interferometry for robust and reliable distance measurements in harsh accelerator environment *Proc. SPIE* **11102**

[3] Campbell M, Hughes B and Veal D 2016 A novel co-ordinate measurement system based on frequency scanning interferometry *Qual. Dig.* **28129**

[4] Deng Z, Liu Z, Jia X and Deng W 2019 Suppression of nonlinear optical frequency sweeping in frequency-scanning interferometry for absolute distance measurement *Proc.SPIE* **11057**

[5] Gilbert S L, Swann W C and Wang C-M 2005 Hydrogen cyanide H13C14N absorption reference for 1530 nm to 1565 nm wavelength calibration–SRM 2519a *NIST Spec. Publ.* **260** 137

[6] Trittler S 2007 *Processing of Interferometric Data* (Heidelberg)

[7] Isa M A, Leach R, Branson D and Piano S 2021 The Effect of Motion Blur on Photogrammetric Measurements of a Robotic Moving Target *Proc. ASPE* 155–160

[8] Ferraguti F, Pertosa A, Secchi C, Fantuzzi C and Bonfè M 2019 A Methodology for Comparative Analysis of Collaborative Robots for Industry 4.0 *2019 Design, Automation & Test in Europe Conference & Exhibition (DATE)* 1070–5

[9] Zhang Z, Liu M, Jiang J, Xia L, Xu X, Zhang W and Zhao Z 2019 Modelling and optimization of a modified sequential multilateration method for three-dimensional coordinate collection *Adv. Mech. Eng.* **11** 1687814019889790

[10] Hughes E B, Wilson A and Peggs G N 2000 Design of a high-accuracy CMM based on multi-lateration techniques *Ann. CIRP* **49** 391–4